

1 **TITLE PAGE**

2 **Convergent relaxation of molecular constraint in herbivores reveals the changing role of liver and**
3 **kidney functions across mammalian diets**

4 Matthew D. Pollard^{1,2*}, Wynn K. Meyer³, and Emily E. Puckett^{1,2}

5 ¹Department of Biological Sciences, University of Memphis, Memphis, TN 38152

6 ²Center for Biodiversity Research, University of Memphis, Memphis, TN 38152

7 ³Department of Biological Sciences, Lehigh University, Bethlehem, PA 18015

8 *Corresponding author

9 **Corresponding author's contact information:**

10 Matthew D. Pollard

11 3700 Walker Avenue, Department of Biological Sciences, University of Memphis, Memphis, TN 38152

12 Phone: 901-216-8184

13 Email: matthew.pollard95@gmail.com

14 **Running Title:** Relaxed molecular constraint during diet evolution

15 **ABSTRACT**

16 Mammalia comprises a great diversity of diet types and associated adaptations. An understanding of the
17 genomic mechanisms underlying these adaptations may offer insights for improving human health.
18 Comparative genomic studies of diet that employ taxonomically restricted analyses or simplified diet
19 classifications may suffer reduced power to detect molecular convergence associated with diet evolution.
20 Here, we used a quantitative carnivory score—indicative of the amount of animal protein in the diet—for
21 80 mammalian species to detect significant correlations between the relative evolutionary rates of genes
22 and changes in diet. We identified six genes—*ACADS*, *CLDN16*, *CPB1*, *PNLIP*, *SLC13A2*, and
23 *SLC14A2*—that experienced significant changes in evolutionary constraint alongside changes in carnivory
24 score, becoming less constrained in lineages evolving more herbivorous diets. We further considered the
25 biological functions associated with diet evolution and observed that pathways related to amino acid and
26 lipid metabolism, biological oxidation, and small molecule transport experienced reduced purifying
27 selection as lineages became more herbivorous. Liver and kidney functions showed similar patterns of
28 constraint with dietary change. Our results indicate that these functions are important for the consumption
29 of animal matter and become less important with the evolution of increasing herbivory. So, genes expressed
30 in these tissues experience a relaxation of evolutionary constraint in more herbivorous lineages.

31

32 **KEYWORDS**

33 adaptation, carnivory, convergent evolution, diet, herbivory, mammal, metabolism

34 **INTRODUCTION**

35 As a diversity of mammalian diets arose from the ancestral insectivorous strategy (Gill et al. 2014),
36 numerous physiological, morphological, and behavioral adaptations also evolved. Understanding the
37 mechanisms of these adaptations may lead to improvements in human health. For example, glucose
38 metabolism in healthy carnivores resembles diabetes in humans and other non-carnivores (Schermerhorn
39 2013). Polar bears are adapted to persistently high blood cholesterol levels (Liu et al. 2014), which have
40 been implicated in human cardiovascular disease (Ference et al. 2017), and some networks underlying polar
41 bear adaptation have been implicated in high-fat dietary adaptations in humans (Fumagalli et al. 2015).
42 Thus, comparative genomic studies of diet offer novel insights for medical advancement. Large-scale
43 comparative genomic resources, consisting of data from hundreds of non-model mammals, have been
44 developed to support such research (Zoonomia Consortium 2020; Christmas et al. 2023).

45 Previous studies identified many genomic changes accompanying adaptations to carnivorous and
46 herbivorous diets. For example, the convergent evolution of herbivory in the giant and red pandas coincided
47 with adaptive molecular evolution of genes associated with the utilization of nutrients that are scarce in
48 bamboo, as well as limb development genes that facilitated growth of the pseudothumb (Hu et al. 2017). In
49 cetaceans, positive selection for proteinases and lipases and loss of pancreatic *RNASE1* expression have
50 been attributed to the evolution of carnivory from a herbivorous ancestor (Wang et al. 2016). Loss of the
51 hormone-receptor pair *INSL5-RXFP4*, which regulates appetite and glucose homeostasis, is thought to be
52 an adaptation to irregular feeding patterns in carnivores (Hecker et al. 2019). Positive selection in carnivores
53 acted on genes associated with successful hunting—such as muscle strength and agility—as well as
54 digestion of fat- and protein-rich foods (Kim et al. 2016).

55 While previous studies provided valuable insights into lineage-specific dietary adaptations, studies that
56 incorporate data encompassing a larger number of taxa can identify mechanisms shared across convergent
57 changes in diet. To date, comparative genomic studies that sampled broadly within mammals have used
58 coarse dietary classification systems, such as herbivore, carnivore, and omnivore (Kim et al. 2016; Hecker

59 et al. 2019; Wu 2022). This results in a loss of important dietary information, as species grouped together
60 differ in the proportions of plant and animal matter consumed and may show divergent adaptations (Pineda-
61 Munoz and Alroy 2014; Grindler and Rabosky 2020; Pollard and Puckett 2022; Reuter et al. 2023). Thus,
62 the power of comparative genomic studies that investigate the molecular mechanisms of dietary adaptation
63 may be reduced.

64 The objectives of our study are two-fold. First, we identify genes that experience convergent changes in
65 evolutionary constraint with increases in carnivory or herbivory across mammals. We accomplish this by
66 detecting significant correlations between gene evolutionary rates and changes in a continuous diet score
67 mapped across a phylogeny of 80 species. Second, we use convergent evolutionary rate shifts to elucidate
68 the biological functions associated with the evolution of increasingly carnivorous or herbivorous diets
69 across Mammalia. Our analyses encompass unprecedented taxonomic breadth and dietary nuance compared
70 to previous comparative genomic studies of diet in mammals.

71 RESULTS

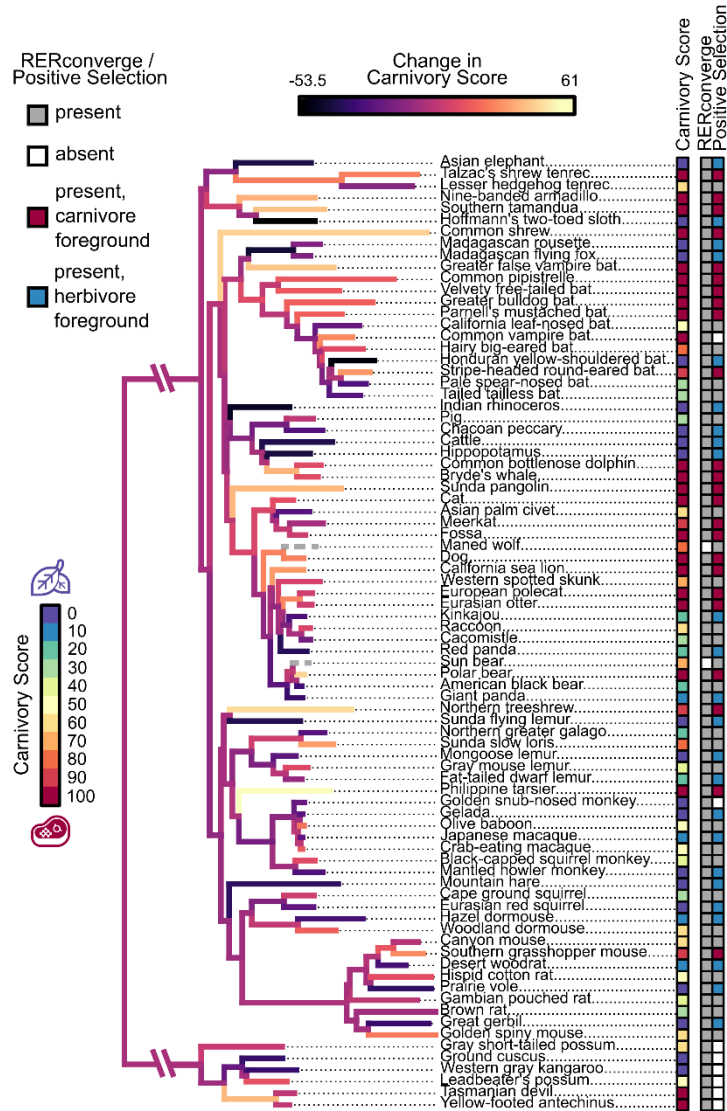
72 *Molecular evolutionary rates associated with dietary change*

73 We generated a carnivory score for each species from the proportion of animal matter in their diet, as
74 reported in the Elton Traits dataset (Wilman et al. 2014). Thus, our study treats invertivorous species as
75 carnivorous. A score of 0 represents a completely herbivorous species, and a score of 100 a completely
76 carnivorous mammal. Due to the structure of Elton Traits, carnivory scores jumped in steps of 10 from 0 to
77 100 (Fig. 1; Supplemental Table S1); we therefore analyzed 11 ordinal bins hereafter called degrees of
78 carnivory.

79 We identified genes that experienced convergent evolutionary constraint or positive selection in association
80 with changes in carnivory across a phylogeny of 80 mammal species (Fig. 1). Of 13,912 genes included in
81 our RERconverge analysis (Kowalczyk et al. 2019), we identified six with a significant negative correlation
82 between relative evolutionary rate (RER) and change in carnivory score (FDR=0.05; Table 1; Fig. 2A;
83 Supplemental Table S3). These significant correlations are a result of convergent rate changes in multiple

84 regions of the phylogeny (Supplemental Fig. S1). A negative correlation represents the following pattern:
85 the greater the decrease in carnivory, the higher the RER of the gene. Decreasing carnivory is proportional
86 to increasing herbivory. Strong negative correlations may be driven by increasingly rapid evolution as the
87 change in carnivory score becomes increasingly negative, slower evolution as the change in carnivory score
88 becomes increasingly positive, or both. A positive correlation represents the opposite pattern: the greater
89 the increase in carnivory (equivalent to decreasing herbivory), the higher the relative rate of evolution of
90 the gene.

91 Negatively correlated genes make a greater contribution to fitness the more carnivory score increases, or a
92 lower contribution the more carnivory score decreases (Kowalczyk et al. 2020). Among genes with this
93 signature, the products of three (*SLC13A2*, *SLC14A2*, and *CLDN16*) are involved in transport or resorption
94 in the kidney, two (*CPB1* and *PNLIP*) are secreted pancreatic enzymes, and one (*ACADS*) is involved in
95 amino acid metabolism (Davis et al. 1991; Pajor 1999; Simon et al. 1999; Andresen et al. 2000; Leung and
96 Morser 2018; Geng et al. 2020). Our analysis had greater power to detect negative associations between
97 RERs and change in carnivory score compared to positive associations (Supplemental Fig. S2).

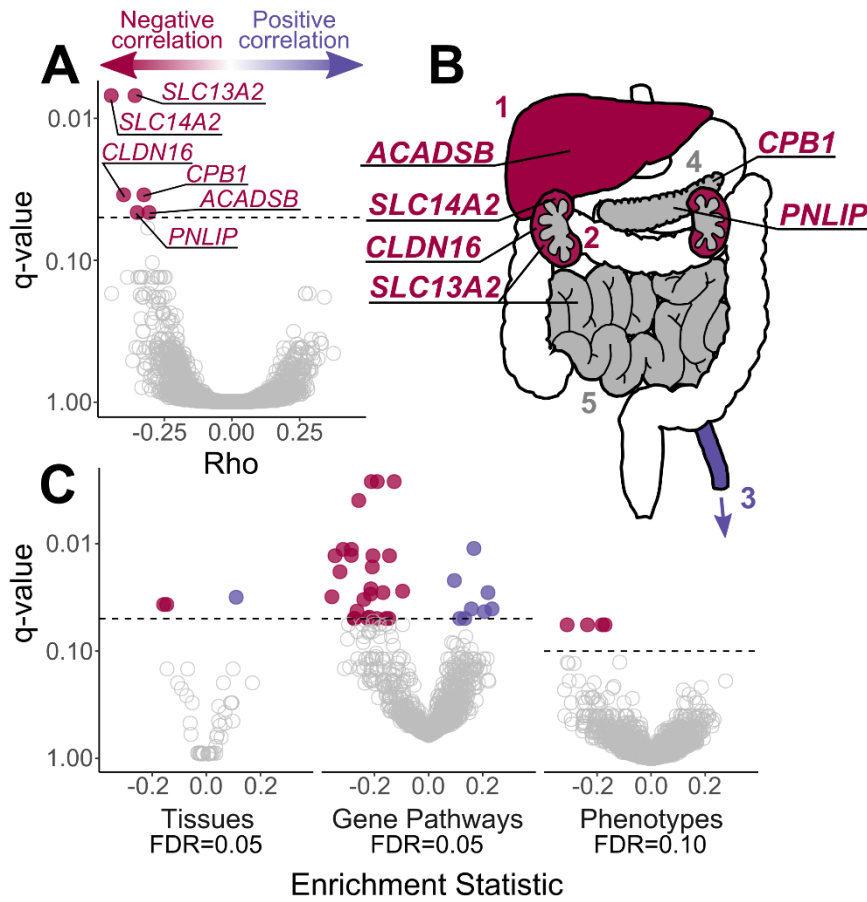


98
99 **Figure 1.** Species selection for comparative genomic analyses of mammalian diet. The carnivory score
100 represents the proportion of the diet composed of animal-based food items for each species, as listed in
101 Elton Traits (Wilman et al. 2014). This score was used as input in our RERconverge analyses and informed
102 selection of foreground species in our tests for positive selection. Branch colors represent the magnitude
103 and direction of change in carnivory score across the phylogeny, as inferred by using fast estimation of
104 maximum likelihood ancestral states (Revell 2012). Bright yellow and dark purple branches indicate
105 increases and decreases in carnivory score, respectively. Gray dashed branches represent species—maned
106 wolf and sun bear—that were not included in our RERconverge analyses and so were not used to estimate
107 change in carnivory score. Branch length represents the average evolutionary rate across all genes for a
108 given branch of the maximum clade credibility phylogeny of Upham et al. (2019), as reported by
109 RERconverge. Most species were included in both the RERconverge and positive selection analyses and
110 are marked as present (gray, red, blue) in the corresponding columns. Species not included in an analysis
111 are marked as absent (white). For the positive selection analyses, species included in the carnivorous
112 (carnivory score ≥ 90) and herbivorous (carnivory score ≤ 10) foregrounds are marked in the corresponding
113 column as red and blue, respectively. Scientific names and carnivory scores are provided for each species
114 in Supplemental Table S1.

Table 1. Genes with evolutionary rates that are significantly associated with change in carnivory score. Permutation *P*-values represent the proportion of 100,000 permutations that produced a stronger correlation with change in carnivory score than the observed value for each gene. Multiple hypothesis testing corrections were performed by generating *Q*-values using Storey's correction method (Storey et al. 2020; FDR=0.05). A negative correlation (Rho) signifies the following pattern: the greater the decrease in carnivory, the higher the rate of evolution of the gene.

Gene	Rho	Parametric <i>P</i> -value	Parametric <i>Q</i> -value	Permutation <i>P</i> -value	Permutation <i>Q</i> -value
<i>SLC14A2</i>	-0.446	1.54 x 10 ⁻⁸	2.14 x 10 ⁻⁴	<1.00 x 10 ^{-5*}	<0.035*
<i>SLC13A2</i>	-0.358	6.94 x 10 ⁻⁶	0.037	<1.00 x 10 ^{-5*}	<0.035*
<i>CLDN16</i>	-0.400	7.93 x 10 ⁻⁶	0.037	1.00 x 10 ⁻⁵	0.035
<i>CPBI</i>	-0.325	8.02 x 10 ⁻⁵	0.150	1.00 x 10 ⁻⁵	0.035
<i>PNLIP</i>	-0.350	1.85 x 10 ⁻⁵	0.065	2.00 x 10 ⁻⁵	0.046
<i>ACADS</i>	-0.306	3.36 x 10 ⁻⁴	0.260	2.00 x 10 ⁻⁵	0.046

* After generating 100,000 null statistics, none produced a stronger correlation with diet than the observed values for *SLC13A2* and *SLC14A2*. However, if the *P*-values are adjusted to the smallest observed non-zero *P*-value (1.00 x 10⁻⁵), they would produce a significant empirical *Q*-value (FDR=0.05).



117

118 **Figure 2.** Top genes and pathways with signatures of diet-associated evolutionary constraint. (A) Genes
 119 identified by RERconverge as having a significant association between relative evolutionary rate and
 120 change in carnivoriness. A negative correlation (Rho) signifies the following pattern: the greater the
 121 decrease in carnivoriness, the higher the rate of evolution of the gene. A positive correlation indicates the
 122 opposite pattern. After 100,000 permutations, six genes showed a significant association, and each evolved
 123 faster in association with decreased carnivoriness (FDR=0.05). (B) Tissues enriched for positive (purple) and
 124 negative (red) correlations, where: 1 = liver, 2 = kidneys, 3 = tibial artery, 4 = pancreas, 5 = small intestine.
 125 Some tissues are annotated with the genes found to be individually significant. The annotated tissues are
 126 the locations of highest expression for those genes in adult humans, according to the Genotype-Tissue
 127 Expression Project (2015). Gray represents tissues that were not significantly enriched but were sites of
 128 strongest expression for individually significant genes. (C) Biological functions showing constraint
 129 associated with change in diet. We used RERconverge to test for enrichment of gene sets representing
 130 tissues (n=50), gene pathways (n=1,290), and abnormal phenotypes (n=3,560). For tissues, two gene sets
 131 were enriched for negative correlations and one set was enriched for positive correlations (Supplemental
 132 Table S4). For gene pathways, 26 gene sets were enriched for negative correlations and 8 sets were enriched
 133 for positive correlations (Supplemental Table S5). For abnormal phenotypes, five gene sets were enriched
 134 for negative correlations (Supplemental Table S6).

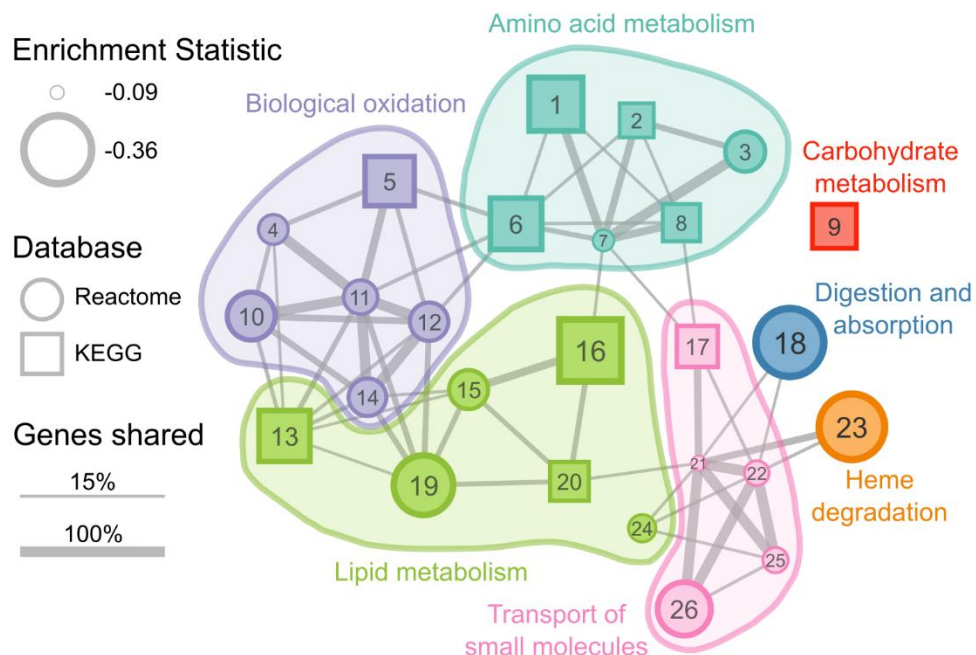
135 Each of the six significant genes is most strongly expressed in the liver, kidneys, pancreas, or small intestine
136 in humans (The GTEx Consortium 2015; Fig. 2B). We performed a gene set enrichment analysis to
137 determine if there was a statistically significant association between change in carnivory score and the rate
138 of evolution of genes expressed in specific tissues (n = 50). Our test showed that the liver and kidney cortex
139 gene sets were significantly enriched for genes that are negatively correlated with change in carnivory score
140 (FDR=0.05; Fig. 2B,C; Tables 2, S4). In contrast, the tibial artery was significantly enriched for genes that
141 are positively correlated with change in carnivory score.

Table 2. Tissues that are significantly enriched for genes associated with change in carnivory score.

Permutation *P*-values represent the proportion of 100,000 permutations that produced a stronger enrichment test statistic than the observed value for each gene set. Multiple hypothesis testing corrections were performed by generating *Q*-values using Storey's correction method (Storey et al. 2020; FDR=0.05). A negative enrichment statistic signifies the following pattern: the greater the decrease in carnivory, the higher the rate of evolution of the gene.

Tissue	Enrichment Statistic	Parametric <i>P</i> -value	Parametric <i>Q</i> -value	Permutation <i>P</i> -value	Permutation <i>Q</i> -value
Tibial Artery	0.111	2.64 x 10 ⁻⁴	0.002	6.30 x 10 ⁻⁴	0.032
Liver	-0.158	1.28 x 10 ⁻¹⁹	6.38 x 10 ⁻¹⁸	0.002	0.037
Kidney Cortex	-0.146	7.42 x 10 ⁻⁷	1.24 x 10 ⁻⁵	0.002	0.037

142
143 We extended our enrichment analysis to 1,290 gene pathways from the Reactome and KEGG databases
144 and identified significant enrichment for 34 pathways (FDR=0.05; Fig. 2C; Supplemental Table S5). Of
145 these pathways, 26 were enriched for genes that are negatively correlated with change in carnivory score.
146 These pathways had functions related to digestion, biological oxidation, transport of small molecules, heme
147 degradation, and metabolism of amino acids, lipids, and carbohydrates (Fig. 3). Eight pathways were
148 enriched for genes that are positively correlated with change in carnivory score. These pathways were
149 associated with cardiovascular disease, cell motility, signaling by anaplastic lymphoma kinase (ALK) in
150 cancer, and signaling by Hippo, NOTCH3, and interleukin 17 (Supplemental Fig. S3). Our gene correlation
151 and pathway enrichment results were robust to changes in species choice and ancestral reconstruction
152 methodology (Supplemental Figs. S4-S5).



153

154 **Figure 3.** Significantly enriched gene pathways ($n=26$) for genes whose evolutionary rates are negatively
 155 correlated with carnivoriness. Each circle or square represents a gene pathway. Circles and squares
 156 represent pathways from the Reactome and KEGG databases, respectively. The size of the shape represents
 157 the magnitude of the difference between the distribution of test statistics for genes in that pathway and the
 158 distribution for all other genes. Larger shapes, representing pathways with more negative correlation
 159 statistics, indicate greater reductions in evolutionary constraint as carnivoriness decreases. The width of
 160 lines connecting pathways represents the proportion of shared genes in the smaller gene set. Colors
 161 represent the broad functional categories that the pathways occupy. 1, Glycine, serine, and threonine
 162 metabolism; 2, Cysteine and methionine metabolism; 3, Sulfur amino acid metabolism; 4, Phase II –
 163 Conjugation of compounds; 5, Drug metabolism – Cytochrome P450; 6, Phenylalanine metabolism; 7,
 164 Metabolism of amino acids and derivatives; 8, Arginine and proline metabolism; 9, Starch and sucrose
 165 metabolism; 10, Metabolic disorders of biological oxidation enzymes; 11, Biological oxidations; 12, Phase
 166 I – Functionalization of compounds; 13, Steroid hormone biosynthesis; 14, Cytochrome P450 – Arranged
 167 by substrate type; 15, Fatty acid metabolism (Reactome); 16, Fatty acid metabolism (KEGG); 17, Proximal
 168 tubule bicarbonate reclamation; 18, Digestion and absorption; 19, Synthesis of bile acids and bile salts via
 169 7alpha-hydroxycholesterol; 20, PPAR signaling pathway; 21, Transport of small molecules; 22, SLC-
 170 mediated transmembrane transport; 23, Heme degradation; 24, Synthesis of phosphatidylcholine; 25,
 171 Transport of bile salts and organic acids, metal ions, and amine compounds; 26, Amino acid transport across
 172 the plasma membrane. A table of results for all gene pathways tested ($n=1,290$) is available in Supplemental
 173 Table S5.

174

175 We performed an enrichment analysis on 3,560 gene sets representing abnormal phenotypes from the
 176 Mammalian Phenotype Ontology (Smith et al. 2005). We identified five phenotypes with significant
 177 enrichment using both raw and permutation-based empirical P -values (FDR=0.1; Fig. 2C; Table 3;

178 Supplemental Table S6). All five gene sets were enriched for genes whose evolutionary rates were
 179 negatively correlated with carnivory score. Two phenotypes—decreased urine osmolality (MP:0002988)
 180 and increased urine calcium level (MP:0005441)—were related to abnormal urine homeostasis, and two
 181 others—abnormal lipid level (MGI:0001547) and abnormal circulating lipid level (MGI:0003949)—were
 182 associated with lipid homeostasis. The abnormal urine homeostasis gene sets shared 8 of 82 total genes,
 183 with 4—*SLC12A1*, *KCTD1*, *SLC4A1*, and *UMOD*—in the 10 top-ranked genes for both gene sets. The
 184 abnormal lipid homeostasis gene sets shared 10 of 134 total genes, with 1 overlapping gene, *BHMT*, in the
 185 top 10 for both sets.

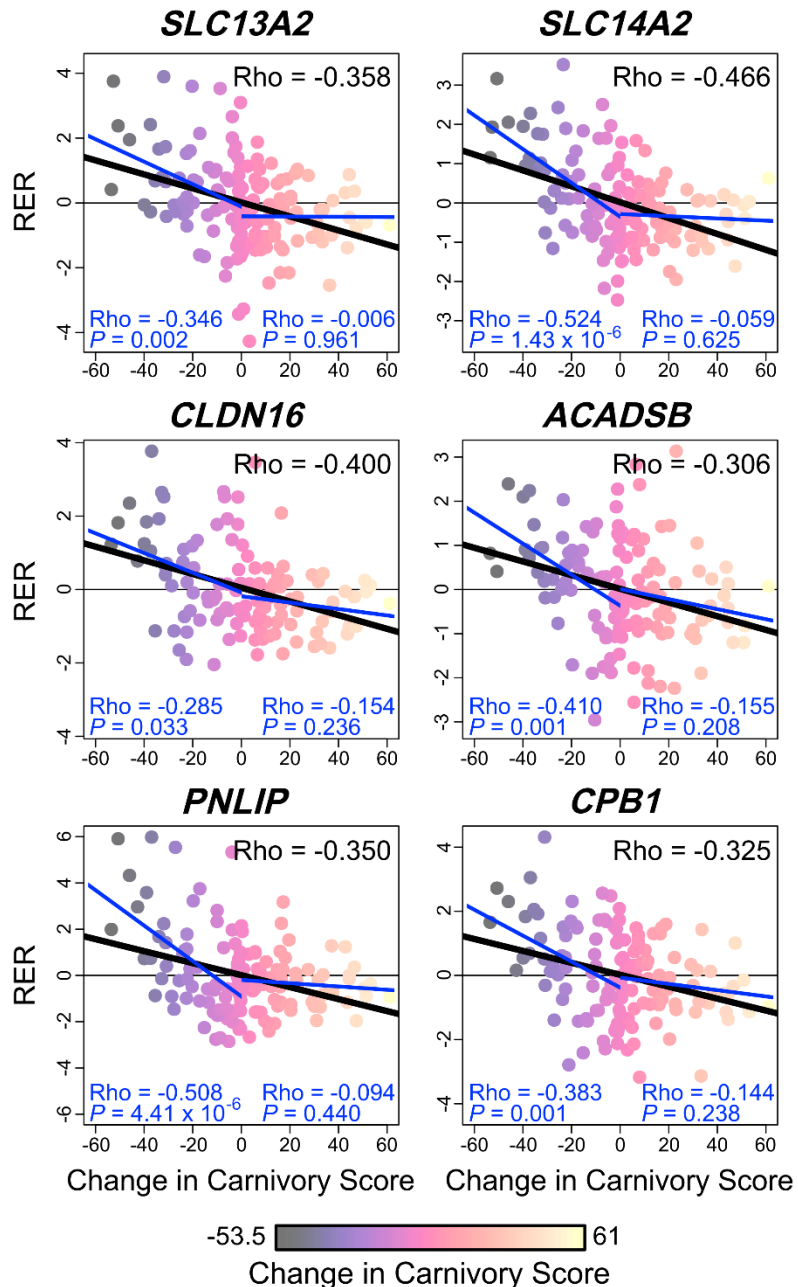
Table 3. Phenotype-based gene sets from the Mammalian Phenotype Ontology that are significantly enriched for genes associated with carnivory score. Permutation *P*-values represent the proportion of 100,000 permutations that produced a stronger enrichment statistic than the observed value for each gene set. Multiple hypothesis testing corrections were performed by generating *Q*-values using Storey's correction method (Storey et al. 2020; FDR=0.1). A negative enrichment statistic signifies the following pattern: the greater the decrease in carnivory, the higher the rate of evolution of the gene.

Phenotype	Enrichment Statistic	Parametric <i>P</i> -value	Parametric <i>Q</i> -value	Permutation <i>P</i> -value	Permutation <i>Q</i> -value
MP:0002223 lymphoid hypoplasia	-0.304	8.60 x 10 ⁻⁴	0.076	<7.00 x 10 ⁻⁵ *	<0.057*
MP:0003949 abnormal circulating lipid level	-0.235	3.30 x 10 ⁻⁵	0.011	7.00 x 10 ⁻⁵ *	0.057*
MP:0001547 abnormal lipid level	-0.170	3.62 x 10 ⁻⁹	1.20 x 10 ⁻⁵	8.00 x 10 ⁻⁵	0.057
MP:0005441 increased urine calcium level	-0.311	7.74 x 10 ⁻⁸	8.53 x 10 ⁻⁵	8.00 x 10 ⁻⁵	0.057
MP:0002988 decreased urine osmolality	-0.181	1.01 x 10 ⁻⁵	0.006	8.00 x 10 ⁻⁵	0.057

* After generating 100,000 null statistics, none produced a stronger correlation with diet than the observed values for MP:0002223. However, if the *P*-values are adjusted to the smallest observed non-zero *P*-value (7.00 x 10⁻⁵), they would produce a significant empirical *Q*-value (FDR=0.1).

186
 187 *Molecular evolutionary rates associated with binary diet classifications*
 188 For the significant genes that we identified in our continuous RERconverge analysis, the negative
 189 correlations between RER and change in carnivory score appeared to be most strongly driven by large RERs
 190 coinciding with the greatest decreases in score (i.e., shifts towards increasing herbivory). Separately

191 calculating Pearson correlation coefficients for increases and decreases in carnivory score supported this,
192 as significant relationships with RER were only identified for decreases in carnivory score (Fig. 4). To
193 determine if this translated to separate relationships with RER at opposing ends of the carnivory score
194 spectrum, we ran binary RER analyses with either the most carnivorous (carnivory score ≥ 90) or most
195 herbivorous (carnivory score ≤ 10) lineages selected as the foreground. Using hypercarnivorous lineages as
196 the foreground, we observed that no genes showed a significant difference in RER between foreground and
197 background lineages (FDR<0.1; Supplemental Table S7). The same was true for the most herbivorous
198 lineages (FDR=0.05); however, we did identify 28 genes with marginally significant associations
199 (FDR<0.1) in this analysis (Supplemental Table S8). This included four of the six genes identified in our
200 analysis of continuous carnivory score—*ACADSB*, *CPB1*, *PNLIP*, and *SLC13A2*—although the strengths
201 of the associations were greater in the continuous analysis. We identified significant enrichment for 78
202 KEGG and Reactome pathways in the herbivore-specific analysis (FDR=0.05), and 21 of these overlapped
203 with the 34 pathways enriched in the continuous analysis (Supplemental Table S9). Pearson correlation
204 coefficients and linear regression analyses indicated that the resulting test statistics of the hyperherbivore
205 analysis were more strongly correlated with those of the continuous analysis than were the test statistics of
206 the hypercarnivore analysis (Supplemental Figs. S6-7).



207

208 **Figure 4.** Relative evolutionary rates (RERs) associated with changes in carnivority score across Mammalia
 209 for six diet-associated genes: *SLC13A2*, *SLC14A2*, *CLDN16*, *ACADSB*, *PNLIP*, and *CPB1*. As in Fig. 1,
 210 light yellow and darker purple points indicate increases and decreases in carnivority score, respectively.
 211 Lines of best fit represent the relationship between RER and change in carnivority score as inferred by linear
 212 regression. Pearson correlation coefficients (Rho) represent the strength and direction of correlations
 213 between RER and change in carnivority score. Black lines of best fit and correlation coefficients (upper right
 214 values) represent the relationship across all changes in carnivority score, as inferred by our continuous
 215 RERconverge analysis. Blue lines, with associated correlations, represent the relationship with RER for
 216 only decreases (left) or increases (right) in carnivority score.

217

218 *Positive selection*

219 We identified 193 and 172 genes that showed significant evidence of positive selection in the most
220 carnivorous and herbivorous species, respectively (FDR=0.05; Supplemental Tables S10, S11). Among the
221 carnivore-specific positively selected genes, we identified enrichment for four Reactome pathways related
222 to *O*-linked glycosylation and one pathway related to pregnenolone biosynthesis (Table 4). The *ADAMTS*
223 (a disintegrin and metalloproteinase with thrombospondin motifs) genes driving the observed enrichment
224 for *O*-linked glycosylation pathways were also components of the only GO Term that was significantly
225 enriched—metallopeptidase activity (GO:0008237; Table 4). We did not identify significant enrichment of
226 any phenotypes, gene pathways, or GO Terms in our list of positively selected genes in herbivores
227 (FDR=0.05).

Table 4. Gene sets enriched for positive selection in the most carnivorous mammals (carnivory score ≥ 90). We did not detect enrichment in the most herbivorous mammals (carnivory score ≤ 10).

Gene Set	# Genes analyzed	Positively selected genes	P-value	Q-value
Reactome Pathways				
<i>O</i> -linked glycosylation	87	<i>ADAMTS5, ADAMTS12, ADAMTS14, ADAMTS20, B4GALT6, CHST4, LARGE2, THSD4</i>	1.83×10^{-5}	0.008
Defective <i>B3GLCT</i> causes Peters-plus syndrome (PpS)	34	<i>ADAMTS5, ADAMTS12, ADAMTS14, ADAMTS20, THSD4</i>	7.70×10^{-5}	0.013
<i>O</i> -glycosylation of TSR domain-containing proteins	35	<i>ADAMTS5, ADAMTS12, ADAMTS14, ADAMTS20, THSD4</i>	8.89×10^{-5}	0.013
Diseases associated with <i>O</i> -glycosylation of proteins	49	<i>ADAMTS5, ADAMTS12, ADAMTS14, ADAMTS20, THSD4</i>	4.50×10^{-4}	0.041
Pregnenolone biosynthesis	12	<i>CYP11A1, FDX2, STARD3NL</i>	4.58×10^{-4}	0.041
GO Terms				
GO:0008237 metallopeptidase activity	158	<i>ADAMTS5, ADAMTS12, ADAMTS14, ADAMTS20, AEBP1, CNDP1, CPZ, PEPD, STAMBPL1, THSD4, TRHDE</i>	5.75×10^{-6}	0.002

228

229 DISCUSSION

230 We used quantitative carnivory scores and a phylogeny of 80 species sampled from the taxonomic and
 231 dietary breadth of Mammalia to identify genes that vary in functional importance based on the relative
 232 proportion of animal-based food sources in a diet. Ours is the first comparative genomic study of diet to
 233 use a quantitative variable and to analyze convergence across so many species. In our analyses of relative
 234 evolutionary rates, we were better able to identify signals of convergent relaxation as carnivory decreases
 235 than the opposite pattern. Our analyses of quantitative carnivory score changes are complementary to but
 236 distinct from methods that search for the most important genes in the most carnivorous or herbivorous
 237 lineages (i.e., without considering all increases and decreases in carnivory score, as in our binary analyses
 238 of RER), and better account for the continuous nature of this complex trait. The main targets of convergence

239 in our study were lipid and amino acid metabolism, biological oxidation, and liver and kidney functions
240 (Fig. 2; Tables 2-4, S5, S6).

241 Many of the signals observed in our analyses appear to be driven most strongly by rapid evolution in
242 increasingly herbivorous lineages (Fig. 4). Indeed, a binary analysis of RERs revealed that many of the
243 biological functions enriched in the continuous analyses were similarly enriched among genes evolving
244 rapidly in hyperherbivores. However, the same was not true in the binary analysis of hypercarnivores
245 (Supplemental Tables S7-S9). The negative correlations likely reflect reduced importance as lineages
246 become increasingly herbivorous. Faster evolution during increases in herbivory represents a convergent
247 relaxation of selection on genes and functions that are important for the consumption of animal matter.
248 Rapid evolution due to positive selection is transient and less likely to be detected by RERconverge than
249 sustained relaxation of purifying selection (Kowalczyk et al. 2020). This is supported by the lack of overlap
250 between our RERconverge and positive selection results (Supplemental Tables S3, S7-8, S10-11).

251 *The roles of liver and kidneys in changing dietary contexts*

252 Multiple lines of evidence support that liver and kidney functions are important for diets that include animal
253 matter and become less important as herbivory increases. Of the six genes identified by our continuous
254 RERconverge analysis as having a significant negative correlation between RER and change in carnivory
255 score, three (*SLC13A2*, *SLC14A2*, and *CLDN16*) and one (*ACADS*) are respectively most strongly
256 expressed in human kidneys and liver (The GTEx Consortium 2015). Further, the kidney cortex and liver
257 gene sets were enriched for negatively correlated genes (Table 2).

258 The changing importance of kidney function as carnivory score increases and decreases may be mediated
259 by its role in the reabsorption and secretion of small molecules. Our enrichment analysis identified several
260 pathways related to small molecule transport, including several containing solute carrier proteins (SLCs)
261 such as the products of *SLC13A2* and *SLC14A2*, that were enriched for genes with negative correlations
262 between RER and change in carnivory score. Many of these pathways take place in the kidneys. The results
263 of our phenotype-specific enrichment analysis also support a diminished role for small molecule

264 transportation in the kidneys of lineages with increasingly herbivorous diets. Of the five MGI phenotype
265 gene sets that were significantly enriched, two of them—decreased urine osmolality (MP:0002988) and
266 increased urine calcium level (MP:0005441)—are related to abnormal urine homeostasis, which is a direct
267 consequence of impaired renal function. Mammals excrete nitrogenous waste in the form of urea, and the
268 urea load that must be excreted each day largely depends on the protein content of an organism's diet. The
269 most carnivorous species produce urine with high urea concentrations due to their protein-rich diets (Liu et
270 al. 2011), suggesting that urea transport plays an important role in these species. This is supported by our
271 finding that the evolutionary rate of *SLC14A2* increases as carnivory score decreases: the urea transporters
272 encoded by this gene are critical to the urea-dependent urine concentrating mechanism (Geng et al. 2020),
273 which may be less important for herbivorous diets with lower protein intakes.

274 Liver function is an important component of evolutionary changes in carnivory score due to its role in
275 amino acid and lipid metabolism. The liver is the only organ in mammals that can completely metabolize
276 most amino acids, and it plays an active role in amino acid synthesis (Hou et al. 2020). Carnivorous diets
277 are rich in proteins and lipids, which represent important energy sources for carnivores. As carnivory
278 declines, these energy sources become less important, so pathways related to their metabolism should be
279 under weaker purifying selection. Among negatively correlated gene pathways, we identified enrichment
280 for genes involved in several processes related to the metabolism of lipids and assorted amino acids,
281 including many that take place within the liver. One such pathway was related to bile acid synthesis
282 (pathway 19, Fig. 3). Bile acids facilitate digestion of dietary fats and allow excess cholesterol to be excreted
283 from the body. Indeed, bile acid synthesis and excretion represent the major mechanisms of cholesterol
284 catabolism and elimination in mammals (Russell 2003). Lipid metabolism pathways may play an important
285 role in maintaining sufficient levels of cholesterol homeostasis in species that consume animal matter.
286 Conversely, lipid homeostasis may be less important in lineages with lipid-poor diets, so constraint relaxes
287 as increasingly herbivorous lineages evolve.

288 Amino acid and lipid metabolism outside of the liver are also associated with change in carnivory. The
289 evolutionary rates of *CPB1* and *PNLIP*—two genes most strongly expressed in the pancreas (The GTEx
290 Consortium 2015)—were significantly negatively correlated with changing carnivory score. A gene for
291 another pancreatic lipase, *PNLIPRP2*, had a marginally significant, negative association with change in
292 carnivory score (Rho=-0.311; $Q=0.059$). The products of *PNLIP* and *PNLIPRP2* are secreted from the
293 pancreas into the small intestine, where they enable efficient digestion of dietary fats (Davis et al. 1991;
294 Lowe 2002). They have been implicated in the dietary switch to carnivory during the evolution of Cetacea,
295 when lipids became a major nutritional component of whales' diets (Wang et al. 2016; Wu 2022). Our
296 results complement these previous findings by highlighting that pancreatic lipases play a reduced role
297 during the evolution of increasing herbivory. Further, another member of this family of pancreatic lipase
298 genes, *PNLIPRP1*, has convergently lost function in multiple herbivorous mammals, suggesting a
299 relaxation of selective constraint in herbivores compared to carnivores (Hecker et al. 2019). The protein
300 encoded by this gene, PL-RP1, shows little to no detectable lipase activity and instead acts as a competitive
301 inhibitor of pancreatic lipase (Lowe 2002). Inactivation of *PNLIPRP1* would therefore enhance fat
302 digestion capacity in herbivores. One may expect that inactivation of *PNLIPRP1* in herbivores may drive a
303 significant negative correlation between RER and change in carnivory score, as this represents an extreme
304 relaxation of selection in herbivores. However, we observed no significant association for *PNLIPRP1*,
305 likely because the gene alignments used in our study do not include pseudogenes. Thus, relaxation of
306 selective pressure leading to pseudogenization cannot be detected using our dataset, and this may have
307 reduced the number of significant associations between RERs and change in carnivory score that we could
308 observe.

309 Metabolism of amino acids and lipids is associated with biological oxidation, and we found that several
310 biological oxidation pathways were enriched for genes negatively correlated with change in carnivory
311 score. This direction of association was unexpected, given the importance of xenobiotic metabolism in
312 herbivores. Many plants employ chemical defenses against herbivory (Berenbaum 1995), and herbivores

313 may overcome these defenses via oxidation (Karban and Agrawal 2002; Dearing et al. 2005). Indeed,
314 Hecker et al. (2019) found that carnivores have lost function of several genes associated with xenobiotic
315 detoxification, as this process is less important in carnivores compared to herbivores. Our binary RER
316 analysis indicated that biological oxidation pathways evolve significantly faster in the most herbivorous
317 lineages (Supplemental Table S9), but we did not detect herbivore-specific positive selection acting on the
318 genes that drove enrichment of these pathways (Supplemental Table S11). This suggests that relaxed
319 selective constraint in increasingly herbivorous lineages is driving our signal, and that a subset of biological
320 oxidation genes may experience reduced purifying selection in herbivores rather than carnivores.

321 Biological oxidation outside the liver is important for dietary adaptation: our positive selection analyses
322 showed that a member of the cytochrome P450 gene superfamily, *CYP11A1*, is positively selected in the
323 most carnivorous species. The protein encoded by *CYP11A1* catalyzes the first stage of steroid hormone
324 synthesis—the production of pregnenolone from cholesterol via oxidation (Payne and Hales 2004). The
325 pregnenolone biosynthesis pathway was enriched in our carnivore-specific positive selection analysis
326 (Table 4), and steroid hormone synthesis showed less constraint as carnivory score decreases (Supplemental
327 Table S5).

328 In summary, our results indicate that as herbivory increased, functions related to the metabolism and
329 elimination of substances found in excess in animal-based foods experienced relaxed purifying selection.
330 The liver and kidneys, which are important sites for these processes, were disproportionately targeted by
331 this relaxation as lineages evolved increasingly herbivorous diets. This drove much of the signal detected
332 by our RERconverge analyses.

333 *Implications of carnivorous adaptation and herbivorous relaxation for human health*

334 Our results offer insights into diet-related diseases in humans and suggest avenues for new medical
335 research. Human dietary maladaptation is not driven by changes in the amount of animal matter consumed
336 *per se*: stable isotopes and archeological evidence indicate that increased meat consumption began early in
337 human evolution (Sponheimer and Lee-Thorp 1999; Domínguez-Rodrigo et al. 2005) and that pre-

338 agricultural diets were more carnivorous than current ones (Eaton and Cordain 1997). Instead, an
339 evolutionarily rapid shift away from pre-agricultural diets in favor of fattier meats and processed foods has
340 increased chronic disease in modern communities (Jew et al. 2009). Our findings help characterize
341 mechanisms of human dietary maladaptation because they highlight metabolic challenges associated with
342 carnivorous diets that are lessened as herbivory increases. These challenges overlap those posed by modern
343 processed diets. For example, adaptations that allow for lipid-rich diets without disease are medically
344 relevant given a global increase in the consumption of high-fat foods in human populations (Kearney 2010).
345 In humans, high intakes of red meat are associated with increased blood cholesterol levels and coronary
346 heart disease (Al-Shaar et al. 2020). These diseases may be related to dysregulation of lipid homeostasis
347 pathways that experienced little selective constraint in our herbivorous primate ancestors (Soligo and
348 Martin 2006). Our phenotype-specific enrichment analysis supports that lipid homeostasis is less
349 functionally important in lineages that increase in herbivory. Two gene sets—abnormal lipid level
350 (MGI:0001547) and abnormal circulating lipid level (MGI:0003949)—are related to lipid homeostasis and
351 were significantly enriched for genes negatively correlated with carnivory score. Thus, the lipid metabolism
352 genes driving our results may be important targets for future studies of dietary maladaptation in humans.
353 A reduction in evolutionary constraint on certain kidney functions as lineages become more herbivorous—
354 and by extension, consume less protein—may be relevant to human health due to the elevated burden of
355 high-protein diets on human renal function. High-protein diets have been linked to kidney damage and
356 reduced renal function in observational human studies (Ko et al. 2020). In other omnivorous mammals,
357 experimental evidence has shown that high protein intake causes kidney inflammation and damage (Jia et
358 al. 2010; Tovar-Palacio et al. 2011). Protein-rich diets have been implicated in kidney stone formation as
359 they increase the excretion of calcium and oxalate into the urine (Robertson et al. 1979). The link between
360 diet and kidney stones offers a plausible connection between *SLC13A2*, carnivory score, and human health,
361 as defects in this gene cause low urinary citrate concentrations, leading to the formation of kidney stones
362 (Okamoto et al. 2007). Defects in another of the significantly negatively correlated genes, *CLDN16*, are

363 associated with elevated urine calcium levels and deposition of calcium salts in the kidneys (Konrad et al.
364 2008).

365 Another pathway with genes that show evidence of relaxation as carnivory score decreases is heme
366 degradation. While nonheme iron is present in both plant- and animal-based foods, heme iron is mainly
367 found in animal tissues (Hurrell and Egli 2010). Species that consume animal tissues ingest excess heme,
368 so heme degradation is an important process in these species. Excess heme intake causes oxidative damage,
369 inflammation, and cell death (Chiabrandi et al. 2014), and has been implicated in several diseases,
370 including type-2 diabetes, coronary heart disease, gut dysbiosis, colitis, and cancers (Bastide et al. 2011;
371 Hooda et al. 2014; Constante et al. 2017). Cancer risk is highest among carnivorous mammals (Vincze et
372 al. 2021), and selection for DNA repair mechanisms in carnivores has been attributed to increased
373 consumption of heme-related reactive oxygen species (Kim et al. 2016). Decreased heme-related disease
374 risk may drive the observed pattern of relaxed evolutionary constraint as lineages become increasingly
375 herbivorous.

376 Carnivore-specific positive selection acting on *O*-linked glycosylation pathways and metalloprotease
377 activity may have relevance to human diabetes. Enrichment for these pathways was primarily driven by
378 four *ADAMTS* genes. *O*-linked glycosylation is a widespread post-translational modification of *ADAMTS*
379 metalloproteases (Wang et al. 2007). The positively selected *ADAMTSs* are associated with extracellular
380 matrix (ECM) assembly and degradation in various biological processes (Glasson et al. 2005; McCulloch
381 et al. 2009; El Hour et al. 2010; Dupuis et al. 2011; Dancevic et al. 2012; Dubail and Apte 2015). In mice,
382 high-fat diets and insulin resistance increase expression of ECM remodeling genes and encourage collagen
383 deposition, leading to fibrosis in tissues such as skeletal muscle, liver, and adipose tissue (Choi et al. 2015;
384 Pincu et al. 2015; Williams et al. 2015). High-fat diets and healthy glucose metabolism that resembles
385 diabetes (Schermerhorn 2013) may increase selective pressure acting on ECM-regulating proteases in
386 carnivores.

387 *Comprehensive sampling elucidated fundamentally important functions*

388 Our analyses sampled the taxonomic and dietary breadth of Mammalia, incorporating genome-wide data
389 from 80 species. The signals of convergent molecular evolution that we detected are driven by multiple
390 instances of dietary convergence across the phylogeny (Fig. 1; Supplemental Fig. S1). We therefore isolated
391 genes and biological functions that differ in importance for carnivory and herbivory in most or all instances
392 that such diets evolved across mammals. Some of our results are concordant with those previously found
393 in studies of fewer species. For example, lipid metabolism has frequently been identified as a target of
394 selection in carnivores (Liu et al. 2014; Kim et al. 2016; Wang et al. 2016). However, our study is the first
395 to emphasize the relevance of kidney and liver functions to evolutionary changes in mammalian carnivory
396 score.

397 By including more species in our analyses, we provide a clearer picture of which diet-specific selection
398 signatures are clade-specific and which are apparent across Mammalia. For example, Kim et al. (2016)
399 found carnivore-specific selection acting on functions such as neuron development, muscle strength, and
400 agility. The authors attribute their findings to agile hunting behaviors. However, we did not detect this
401 selection in our broader analysis. Some carnivores in our expanded sampling are not agile predators and
402 are unlikely to have experienced selection on these functions. For example, Bryde's whale was included in
403 our analyses and feeds on zooplankton with limited movement capabilities (Izadi et al. 2022). Bryde's
404 whale does not require the same agility while hunting as the carnivorans, orca, and Tasmanian devil that
405 were analyzed by Kim et al. (2016).

406 *Increases in herbivory led to convergent relaxation more often than constraint*

407 The evolutionary history of mammalian diet offers a potential explanation for why many of our results were
408 driven by molecular changes that co-occurred with evolution towards herbivory. The ancestral mammalian
409 diet was insectivorous (Gill et al. 2014) and would be treated as completely carnivorous in our study. Thus,
410 less carnivorous diets represent derived states that are likely associated with great molecular and phenotypic
411 change as entirely new dietary adaptations arise. In contrast, lineages that increase in carnivory are returning

412 to a state more like the ancestral condition, potentially leading to smaller shifts in gene evolutionary rates.
413 This may lead to a stronger relationship between gene evolutionary rates and diet for decreases in carnivory
414 score.

415 While the history of mammalian diet may help explain the stronger relationship with gene evolutionary
416 rates as carnivory score decreases, it does not explain why the signal of evolutionary constraint was much
417 weaker than relaxation in this direction of dietary change (Supplemental Fig S2, Supplemental Tables S3-
418 6, S8-9). The weaker signal may be a consequence of the base level of constraint that acts on protein
419 evolution (Worth et al. 2009). Given that proteins already experience some level of constraint, it is likely
420 harder to detect further reductions in an already low evolutionary rate compared to increases.

421 The weaker signal we observed in genes with positive correlations than in those with negative correlations
422 could also indicate that constraint on coding sequence is less predictable during adaptation to increased
423 herbivory than to increased carnivory. Low predictability may be mediated by diverse digestive strategies
424 in herbivores, and by greater variation in the nutrient composition of plant-based foodstuffs. Herbivores
425 can be categorized by the method of microbial fermentation employed to digest plant material. Foregut and
426 hindgut fermenters differ in the volume and nutritional quality of plant matter that they can consume
427 (Alexander 1993), and this places different morphophysiological constraints on each strategy (Clauss et al.
428 2003). Fruits, seeds, and foliage differ in the proportions of protein, lipids, and structural versus non-
429 structural carbohydrates that they contain (Jordano 2000). Thus, the diets of frugivores, granivores, and
430 folivores differ in digestibility and energy content, and each strategy will employ a different suite of
431 adaptations to reflect this. This diversity within herbivory may help explain our observation of less
432 convergent constraint acting during evolution of increasing herbivory than convergent relaxation.

433 *Pathways enriched for positively correlated genes have unresolved links to diet evolution*

434 The relevance to diet or health of pathways containing genes that are positively correlated with change in
435 carnivory score is generally less obvious than those with the opposite pattern. These pathways may
436 represent understudied components of dietary adaptation. For example, Hippo signaling integrates signals

437 from multiple sources to regulate cell proliferation and differentiation, and can influence and be influenced
438 by the metabolism of glucose, lipids, and amino acids (Ibar and Irvine 2020). Given that multiple metabolic
439 cues are integrated into Hippo signaling, it is unclear why genes in this pathway experience changes in
440 constraint as carnivory score increases and decreases. NOTCH3 plays an important role during vascular
441 development and in continued vascular functioning of adult organisms (Domenga et al. 2004; Loerakker et
442 al. 2018; Hosseini-Alghaderi and Baron 2020). Given this, enrichment for NOTCH3 signaling may be
443 related to a shared selective pressure that drives enrichment of the tibial artery gene set in the same direction
444 (Table 2). However, it is unclear why vascular function would be associated with changing carnivory score.
445 ALK activation is involved in the development of many cancers (Della Corte et al. 2018), but its function
446 beyond cancer is not as well understood. It is thought to play a role in nervous system development (Palmer
447 et al. 2009), but expression has also been detected in the small intestine and colon (Morris et al. 1994).
448 More recently, ALK signaling was implicated in regulating energy expenditure and weight gain (Orthofer
449 et al. 2020), so it might play an important, unidentified role in diet regulation, and further study could
450 elucidate its relevance.

451 Despite limited signal and unclear relevance for many pathways enriched for positively correlated genes,
452 one pathway stood out as having a clear connection to diet evolution. The association of interleukin 17
453 (IL17) signaling with changing carnivory score may reflect IL17's role in gut microbiome regulation. IL17
454 encourages the production of antimicrobial proteins and the migration of neutrophils into infected intestinal
455 mucosa, maintains intestinal barrier integrity, and limits gut dysbiosis (Aujila et al. 2007; Ishigame et al.
456 2009; Cao et al. 2012; Pérez et al. 2018). Gut microbiomes are essential for herbivores. The plants
457 consumed by herbivores comprise complex polysaccharides that cannot be digested by mammalian
458 enzymes. However, microorganisms in the herbivore gut can ferment these compounds to produce
459 metabolites that are used easily by their host. The importance of microorganisms for plant consumption has
460 led to convergence in gut microbiota across mammalian herbivores, while those of carnivores are highly

461 variable (Muegge et al. 2011; Zoelzer et al. 2021). As gut microbes are necessary for successful herbivory,
462 evolutionary constraint should act on gut homeostasis pathways as herbivory increases.

463 *Limitations of the study and suggestions for future work*

464 Although RERconverge has demonstrated success in associating gene RERs with the evolution of
465 continuous traits (Kowalczyk et al. 2020), the underlying model has some limitations. When analyzing a
466 continuous trait, RERconverge does not by default associate raw trait values with gene RERs because this
467 would lead to phylogenetic dependence among branches. Instead, RERconverge calculates trait change
468 between a descendent and its ancestor (Kowalczyk et al. 2019). It detects genes with RERs that are
469 significantly correlated with trait change, as such genes are crucial to the convergent evolution of that trait.
470 However, in lineages that remain stationary in trait space following an ancestral transition, trait-associated
471 genes may remain under continued evolutionary constraint or relaxation, despite no change in the trait.
472 Consequently, the model may fail to implicate these genes as important and may instead identify genes that
473 are important only for trait transitions and not in maintaining a phenotype once it has evolved. By
474 quantifying the robustness of our results to species removal (Supplemental Fig. S4), we demonstrated that
475 the signals we detected were not impacted by specific lineages, regardless of whether they represent areas
476 of the phylogeny with active or stationary diet evolution. Thus, we can be confident that the genes we
477 identified play important roles in adaptation to changes in carnivory score across Mammalia. However, we
478 may have had insufficient power to detect additional diet-associated genes.

479 We also showed congruence between our continuous and binary analyses of RER (Supplemental Tables
480 S3, S5, S8, S9). When implemented with lineages subsequent to transitions as foreground, binary
481 RERconverge identified genes involved in transition to and maintenance of a foreground trait. However,
482 this is at the cost of ignoring small changes in the trait that may be evolutionarily relevant. The ability to
483 integrate changes in dietary traits may explain why our continuous analyses returned significant
484 associations at an FDR of 0.05 while the binary analyses did not (Supplemental Tables S3, S7-8). For future
485 studies of continuous traits, it may be preferable to develop a version of RERconverge that calculates

486 changes in RER, rather than correlating trait change with raw RER values. This would negate the issue
487 caused by lineages with extreme yet unchanging trait values, because important genes would show little
488 change in RER on the corresponding branches.

489 Although our consideration of degree of carnivory as a quantitative trait expands upon prior studies that
490 define diet categorically, this definition has limitations as well. Elton Traits, used to construct our carnivory
491 score, was built primarily from qualitative summarizations of existing literature written in Walker's
492 Mammals of the World (Nowak 1999). While our carnivory score is likely accurate for extreme carnivores
493 and herbivores, accuracy of intermediate scores may vary based on how reliably the diets were coded within
494 Elton Traits. Inaccurate diet classifications for species with intermediate phenotypes would introduce noise
495 into the inference of how carnivory score evolves on the phylogeny, ultimately reducing the power of our
496 RERconverge analyses. Nevertheless, Elton Traits data has been used effectively to address several
497 questions in ecology and evolution, such as the influence of diet on the evolution of mammalian gut
498 microbiomes (Groussin et al. 2017), the effect of diet on species' responses to climate change (Buckley et
499 al. 2018), and the decline of ecological and functional diversity over time (Cooke et al. 2019; Brodie et al.
500 2021). The demonstrated efficacy of Elton Traits in prior works suggests that it can provide valuable data
501 for our study, despite these limitations.

502 Our analyses may be impacted by a mismatch between carnivory score and genomic data for the dog, *Canis*
503 *lupus*. The Elton Traits entry for *C. lupus* represents the hypercarnivorous wolf, while the genetic data was
504 obtained from a domesticated dog. During early domestication, the dog adapted to a more omnivorous diet
505 (Axelsson et al. 2013). A carnivory score of 100 does not accurately reflect the diet of modern dogs.
506 However, this mismatch should not strongly impact our results. Dogs certainly possess some adaptations
507 to omnivory, but their domestication occurred relatively recently (~15,000 years; Savolainen et al. 2002;
508 Pang et al. 2009). Thus, signals of selection for carnivory may be detectable in dogs, given the longer
509 evolutionary history of hypercarnivory within the lineage. Regardless of whether there is a mismatch, it is
510 unlikely that any significant signal will be singularly mediated by the branch leading to dog.

511 Our quantitative carnivory score more accurately reflects the biologically continuous nature of diet and
512 leads to less information loss compared to typical categorical classifications, but it still does not capture all
513 dietary variation. While the diets of strictly herbivorous species may be identical in that they do not include
514 animal matter, they differ in nutritional composition based on the plant-based foodstuffs consumed—seeds,
515 fruit, leaves, or other plant matter. The same is true of carnivorous species. For example, the blood-based
516 diet of the common vampire bat differs from other carnivores included in our study by being vitamin- and
517 lipid-poor (Mendoza et al. 2018). Studies that separate nutritional composition from the carnivory-
518 herbivory axis of diet variation may detect signals of selection that would otherwise be masked, and can
519 test the hypotheses of earlier comparative genomic analyses of diet. For example, a recent study considered
520 fat intake and found evidence to support an earlier hypothesis that functional loss of *PNLIPRP1* in
521 herbivores is associated with low fat consumption (Hecker et al. 2019; Wagner et al. 2022). Insights from
522 comparative genomic studies of diet composition will produce important insights for medical advancement
523 in the future.

524 **METHODS**

525 *Preparation of dietary data*

526 To create a continuous categorization of diet, we obtained data from the Elton Traits mammal dataset
527 (Wilman et al. 2014). Data compiled in Elton Traits came primarily from Walker's Mammals of the World
528 (Nowak 1999), which describes species' diets based on summaries of existing literature. Qualitative
529 descriptions of dietary preferences were translated by the Elton Traits authors into numerical values
530 representing the proportion of diet comprising numerous food types. In this study, we generated a carnivory
531 score for each species by summing the proportions of vertebrates and invertebrates in their diet.

532 *Study species and gene alignments*

533 For our analyses of relative evolutionary rates (RERs), we selected 80 species that encompass the
534 taxonomic and dietary breadth of therian mammals (Fig. 1; Supplemental Table S1). We filtered multiple
535 codon alignments that were generated with TOGA and MACSE v2 by the Zoonomia Consortium (2020;

536 Ranwez et al. 2018; Kirilenko et al. 2023) using the methodology described in Wirthlin et al. (2024; see
537 Supplemental Material). We then pruned the alignments so that they included only our chosen species, and
538 removed sequences that did not cover 50% of the total aligned sequence length. For alignments that
539 included more than one sequence per species, we retained the sequence with the highest percent identity to
540 human. We only analyzed alignments with sequences that survived filtering for at least 60 target species.
541 Our filtering reduced the number of genes analyzed from 17,439 to 15,117. An overrepresentation analysis
542 of Gene Ontology (GO) terms indicated that the unanalyzed genes were predominantly associated with
543 DNA assembly and organization, perception of chemical stimuli, and gene silencing (Supplemental Table
544 S2). These nucleotide alignments were translated to amino acid alignments for use with RERconverge.

545 *Associating relative evolutionary rates with the evolution of diet*

546 We used RERconverge in R (Kowalczyk et al. 2019; R Core Team 2023) to identify genes with consistent
547 changes in evolutionary rate associated with the evolution of the quantitative carnivoriness score. RERs reveal
548 deviation in evolutionary rate along a specific branch of the phylogeny, based on genome-wide and gene-
549 specific expectations. A highly positive RER may indicate positive selection or relaxation of constraint. A
550 highly negative RER indicates that increased constraint has led to fewer substitutions than expected. As we
551 implemented it, RERconverge estimates the correlation between RER and change in a continuous
552 phenotype across a phylogeny. A significant negative correlation between RER and change in carnivoriness
553 score corresponds to slower evolution the more carnivoriness increases, and/or faster evolution the more
554 carnivoriness decreases. Increased evolutionary constraint is associated with slower molecular evolution and
555 implies that the gene contributes more to fitness under a particular phenotypic condition (Kowalczyk et al.
556 2020).

557 We used the *estimatePhangornTreesAll* wrapper function from RERconverge, which utilizes a maximum
558 likelihood approach implemented in phangorn (Schliep 2011), to calculate branch lengths for each gene
559 while fixing the topology of the gene trees to match the maximum clade credibility phylogeny of Upham
560 et al. (2019). These trees were used as input for the RERconverge analyses alongside our carnivoriness scores.

561 We winsorized the RERs of each gene so that the three most extreme values at each end were set to that of
562 the next most extreme RER. This minimized the influence of outliers. We implemented the default branch
563 length filtering in RERconverge, setting the shortest 5% of branches across all gene trees to N/A. This
564 resulted in an additional 1,205 genes being filtered for having fewer than 60 branches remaining in the tree,
565 leaving 13,912 remaining genes in this analysis.

566 To evaluate confidence in gene-trait associations inferred by RERconverge, we used a phylogenetically
567 restricted permutation strategy ('permulations'; Kowalczyk et al. 2020; Saputra et al. 2021). We randomly
568 simulated carnivory scores for each species 100,000 times using a Brownian motion model of evolution.
569 Then for each simulated set of values, the observed carnivory scores were assigned to species based on the
570 ranks of the simulated scores. We used these shuffled phenotype sets to calculate gene-trait associations
571 using RERconverge, generating 100,000 null statistics per gene. We calculated a new, empirical *P*-value
572 for each gene-trait association based on the proportion of null statistics that are equally or more extreme
573 than the observed statistic for that association. We corrected for multiple hypothesis testing using Storey's
574 correction method (Storey et al. 2020; FDR=0.05). Using the Mann-Whitney *U* test for enrichment available
575 in RERconverge, we identified biological functions associated with the evolution of diet. We constructed
576 tissue-specific gene sets from the Genotype-Tissue Expression Project (GTEx; The GTEx Consortium
577 2015) data, defining tissue-specificity following the strategy of Jain and Tuteja (2019). Briefly, tissue-
578 specific genes were identified as those with expression levels of at least one transcript per million (TPM)
579 that were significantly higher (at least five-fold) in up to seven tissues compared to all others. We tested for
580 tissue-specific enrichment using these gene sets, gene pathway enrichment using KEGG and Reactome
581 pathways from MSigDB (Liberzon et al. 2011), and enrichment for abnormal phenotypes using gene sets
582 from the Mammalian Phenotype (MP) Ontology (Smith et al. 2005).

583 We checked the robustness of our RERconverge results to species choice and ancestral reconstruction
584 method (see Supplemental Material). We also compared our results to those produced using binary
585 classifications of diet (see Supplemental Material).

586 *Positive selection associated with the evolution of carnivory or herbivory*

587 We tested each gene for positive selection via branch-site models (branch-site neutral versus branch-site
588 selection) using codeml from PAML (Yang 2007), as implemented in BASE (Forni et al. 2021). We also
589 used BUSTED from the HyPhy software suite (Murrell et al. 2015; Pond et al. 2020). These models test for
590 positive selection in a group of foreground species chosen *a priori*. Terminal branches leading to species
591 with carnivory scores ≥ 90 (n=25) and ≤ 10 (n=24) were selected as foreground for carnivory- and herbivory-
592 specific analyses, respectively (Fig. 1; Supplemental Table S1). Select species with carnivory scores of
593 20—specifically the red panda and kinkajou—were included in the herbivore foreground despite relatively
594 high carnivory scores because they are considered in the broader literature to be primarily herbivorous
595 (Yonzon and Hunter 1991; Julien-Laferrière 1999; Kays 1999; Pradhan et al. 2001; Panthi et al. 2012).

596 As in our RERconverge analyses, we obtained nucleotide alignments for each gene from Zoonomia and
597 applied the same filtering steps. However, due to an updated data release from Zoonomia, the alignment
598 files used for positive selection tests differed from those obtained for the RERconverge analysis.
599 Specifically, the second set included the maned wolf and sun bear, but did not include marsupials. Given
600 that the maned wolf and sun bear have carnivory scores that differ from their closely related species (Fig.
601 1), we retained them in these analyses to increase our representation of dietary diversity across the
602 phylogeny.

603 PAML branch-site models do not test for the absence of positive selection in background species, so these
604 tests alone do not identify genes experiencing positive selection in association with a trait of interest
605 (Kowalczyk et al. 2021). To confirm that our significant branch-site results corresponded to foreground-
606 specific positive selection, we removed the foreground species and tested for tree-wide positive selection
607 using site models (M1a versus M2a) in PAML. Only genes detected as positively selected by the branch-
608 site model and not the site model with foreground species excluded were retained (Supplemental Fig. S8).

609 We employed a conservative strategy to generate final lists of positively selected genes. To account for the
610 impact of gene tree discordance on our results (Mendes and Hahn 2016), we performed positive selection

611 analyses using gene trees and the fixed species tree. We used RAxML v8.2.12 (Stamatakis 2014) with the
612 GTRGAMMA1 nucleotide substitution model to generate gene trees. We only considered a gene to have
613 experienced diet-associated positive selection when it produced a significant result in both our codeml and
614 BUSTED analyses, and if this result persisted when using the gene tree and the species tree (Supplemental
615 Fig. S8). As an additional filtering step, we checked that the signals of positive selection returned by codeml
616 and BUSTED were not caused by relaxation of selection by using RELAX (Wertheim et al. 2015), and
617 excluded any genes showing significant relaxation from our final gene lists (Supplemental Fig. S8). We
618 used overrepresentation analyses to test our final lists for enrichment of GO terms, gene pathways from the
619 Reactome and KEGG databases, phenotypes from the MP Ontology, and our tissue-specific gene sets using
620 clusterProfiler and ReactomePA (Yu et al. 2012; Yu and He 2016). For all overrepresentation analyses, we
621 used human annotation databases.

622 **DATA ACCESS**

623 All nucleotide and amino acid alignments used in this study were generated via TOGA annotation of
624 orthologous genes by the Zoonomia Consortium (<https://zoonomiaproject.org/the-data/>;
625 https://genome.senckenberg.de/download/TOGA/human_hg38_reference/MultipleCodonAlignments/).
626 The filtered nucleotide and amino acid alignments generated in this study are available on FigShare
627 (<https://doi.org/10.6084/m9.figshare.25695762>). Carnivory scores for species included in this study are
628 available in Supplemental Table S1. All RERconverge and positive selection results generated in this study
629 are available in Supplemental Tables S3-11. All code used for data processing and analysis are available
630 on GitHub (<https://github.com/mdpllard/carnivory-genes>), FigShare, and as Supplemental Code. The
631 tissue- and mouse phenotype-specific gene sets generated in this study are available on GitHub, FigShare,
632 and in the Supplemental Code.

633 **COMPETING INTEREST STATEMENT**

634 The authors declare that they have no competing interests.

635 **ACKNOWLEDGEMENTS**

636 We thank the administrators of the University of Memphis High Performance Computing (HPC) facilities
637 for support during this study. We thank the three anonymous reviewers for their insightful feedback on the
638 submitted manuscript, Amanda Kowalczyk and Ruby Redlich for developing the ‘getPermsBinaryFudged’
639 function to improve permutation speed, and Emily Kopania and Michael Tene for helpful discussions. This
640 material is based upon work supported by the National Science Foundation under Grant No. 2233124 to
641 WKM.

642 **AUTHOR CONTRIBUTIONS**

643 MDP and WKM performed data pre-processing. MDP analyzed the data and interpreted results with EEP
644 and WKM. MDP wrote the manuscript. EEP and WKM edited the manuscript. EEP supervised the study.

645 **REFERENCES**

646 Al-Shaar L, Satija A, Wang DD, Rimm EB, Smith-Warner SA, Stampfer MJ, Hu FB, and Willett WC.
647 2020. Red meat intake and risk of coronary heart disease among US men: prospective cohort study. *BMJ*
648 **371**: m4141.

649 Alexander RM. 1993. The relative merits of foregut and hindgut fermentation. *J Zool* **231**: 391-401.

650 Andresen BS, Christensen E, Corydon TJ, Bross P, Pilgaard B, Wanders RJA, Ruiter JPN, Simonsen H,
651 Winter V, Knudsen I *et al.* 2000. Isolated 2-methylbutyrylglycinuria caused by short/branched-chain acyl-
652 CoA dehydrogenase deficiency: identification of a new enzyme defect, resolution of its molecular basis,
653 and evidence for distinct acyl-CoA dehydrogenases in isoleucine and valine metabolism. *Am J Hum Genet*
654 **67**: 1095-1103.

655 Aujila SJ, Dubin PJ, and Kolls JK. 2007. Th17 cells and mucosal host defense. *Semin Immunol* **19**: 377-
656 382.

657 Axelsson E, Ratnakumar A, Arendt M-L, Maqbool K, Webster MT, Perloski M, Liberg O, Arnemo JM,
658 Hedhammer Å, and Lindblad-Toh K. 2013. The genomic signature of dog domestication reveals adaptation
659 to a starch-rich diet. *Nature* **495**: 360-364.

660 Bastide NM, Pierre FHF, and Corpet DE. 2011. Heme iron from meat and risk of colorectal cancer: a meta-
661 analysis and a review of the mechanisms involved. *Cancer Prev Res* **4**: 177-184.

662 Berenbaum MR. 1995. The chemistry of defense: theory and practice. *PNAS* **92**: 2-8.

663 Brodie JF, Williams S, and Garner B. 2021. The decline of mammal functional and evolutionary diversity
664 worldwide. *PNAS* **118**: e1921849118.

665 Buckley LB, Khalil I, Swanson DL, and Hof C. 2018. Does metabolism constrain bird and mammal ranges
666 and predict shifts in response to climate change? *Ecol Evol* **8**: 12375-12385.

667 Cao AT, Yao S, Gong B, Elson CO, and Cong Y. 2012. Th17 cells upregulate polymeric Ig receptor and
668 intestinal IgA and contribute to intestinal homeostasis. *J Immunol* **189**: 4666-4673.

669 Chiabrand D, Vinchi F, Fiorito V, Mercurio S, and Tolosano E. 2014. Heme in pathophysiology: a matter
670 of scavenging, metabolism and trafficking across cell membranes. *Front Pharmacol* **5**: 61.

671 Choi M-S, Kim Y-J, Kwon E-Y, Ryoo JY, Kim SR, and Jung UJ. 2015. High-fat diet decreases energy
672 expenditure and expression of genes controlling lipid metabolism, mitochondrial function and skeletal
673 system development in the adipose tissue, along with increased expression of extracellular matrix
674 remodelling- and inflammation-related genes. *Brit J Nutr* **113**: 867-877.

675 Christmas MJ, Kaplow IM, Genereux DP, Dong MX, Hughes GM, Li X, Sullivan PF, Hindle AG, Andrews
676 G, Armstrong JC *et al.* 2023. Evolutionary constraint and innovation across hundreds of placental
677 mammals. *Science* **380**: eabn3943.

678 Clauss M, Frey R, Kiefer B, Lechner-Doll M, Loehlein W, Polster C, Rössner GE, and Streich WJ. 2003.
679 The maximum attainable body size of herbivorous mammals: morphophysiological constraints on foregut,
680 and adaptations of hindgut fermenters. *Oecologia* **136**: 14-27.

681 Constante M, Fragoso G, Calvé A, Samba-Mondonga M, and Santos MM. 2017. Dietary heme induces gut
682 dysbiosis, aggravates colitis, and potentiates the development of adenomas in mice. *Front Microbiol* **8**:
683 1809.

684 Cooke RSC, Eigenbrod F, and Bates AE. 2019. Projected losses of global mammal and bird ecological
685 strategies. *Nat Commun* **10**: 2279.

686 Dancevic CM, Fraser FW, Smith AD, Stupka N, Ward AC, and McCulloch DR. 2012. Biosynthesis and
687 expression of a disintegrin-like and metalloproteinase domain with thrombospondin-1 repeats-15. *J Biol
688 Chem* **288**: 37267-37276.

689 Davis RC, Diep A, Hunziker W, Klisak I, Mohandas T, Schotz MC, Sparkes RS, and Lusis AJ. 1991.
690 Assignment of human pancreatic lipase gene (PNLIP) to chromosome 10q24-q26. *Genomics* **11**: 1164-
691 1166.

692 Dearing MD, Foley WJ, and McLean S. 2005. The influence of plant secondary metabolites on the
693 nutritional ecology of herbivorous terrestrial vertebrates. *Annu Rev Ecol Evol S* **36**: 169-189.

694 Della Corte CM, Viscardi G, Di Liello R, Fasano M, Martinelli E, Troiani T, Ciardiello F, and Morgillo F.
695 2018. Role and targeting of anaplastic lymphoma kinase. *Mol Cancer* **17**: 30.

696 Domenga V, Fardoux P, Lacombe P, Monet M, Maciazek J, Krebs LT, Klonjkowski B, Berrou E,
697 Mericskay M, Li Z *et al.* 2004. Notch3 is required for arterial identity and maturation of vascular smooth
698 muscle cells. *Gene Dev* **18**: 2730-2735.

699 Domínguez-Rodrigo M, Pickering TR, Semaw S, and Rogers MJ. 2005. Cutmarked bones from Pliocene
700 archaeological sites at Gona, Afar, Ethiopia: implications for the function of the world's oldest stone tools.
701 *J Hum Evol* **48**: 109-121.

702 Dubail J, and Apte SS. 2015. Insights on ADAMTS proteases and ADAMTS-like proteins from mammalian
703 genetics. *Matrix Biol* **44-46**: 24-37.

704 Dupuis LE, McCulloch DR, McGarity JD, Bahan A, Wessels A, Weber D, Diminich AM, Nelson CM,
705 Apte SS, and Kern CB. 2011. Altered versican cleavage in ADAMTS5 deficient mice; a novel etiology of
706 maxomatous valve disease. *Dev Biol* **357**: 152-164.

707 Eaton SB, and Cordain L. 1997. Evolutionary Aspects of Diet: Old Genes, New Fuels. In *Nutrition and*
708 *Fitness: Evolutionary Aspects, Children's Health, Programs and Policies*. (ed. Simopoulos AP), pp. 26-37.
709 Karger, Basel.

710 El Hour M, Moncada-Pazos A, Blacher S, Masset A, Cal S, Berndt S, Detilleux J, Host L, Obaya AJ,
711 Maillard C *et al.* 2010. Higher sensitivity of *Adams12*-deficient mice to tumor growth and angiogenesis.
712 *Oncogene* **29**: 3025-3032.

713 Ference BA, Ginsberg HN, Graham I, Ray KK, Packard CJ, Bruckert E, Hegele RA, Krauss RM, Raal FJ,
714 Schunkert H *et al.* 2017. Low-density lipoproteins cause atherosclerotic cardiovascular disease. 1. Evidence
715 from genetic, epidemiologic, and clinical studies. A consensus statement from the European Atherosclerosis
716 Society Consensus Panel. *Eur Heart J* **28**: 2459-2472.

717 Forni G, Ruggieri AA, Piccinini G, and Luchetti A. 2021. BASE: a novel workflow to integrate
718 nonubiquitous genes in comparative genomics analyses for selection. *Ecol Evol* **11**: 13029-13035.

719 Fumagalli M, Moltke I, Grarup N, Racimo F, Bjerregaard P, Jørgensen ME, Korneliussen TS, Gerbault P,
720 Skotte L, Linneberg A *et al.* 2015. Greenlandic Inuit show genetic signatures of diet and climate adaptation.
721 *Science* **349**: 1343-1347.

722 Geng X, Zhang S, He J, Ma A, Li Y, Li M, Zhou H, Chen G, and Yang B. 2020. The urea transporter UT-
723 A1 plays a predominant role in a urea-dependent urine-concentrating mechanism. *J Biol Chem* **295**: 9893-
724 9900.

725 Gill PG, Purnell MA, Crumpton N, Robson Brown K, Gostling NJ, Stampanoni M, and Rayfield EJ. 2014.
726 Dietary specialization and diversity in feeding ecology of the earliest stem mammals. *Nature* **512**: 303-305.

727 Glasson SS, Askew R, Sheppard B, Carito B, Blanchet T, Ma H-L, Flannery CR, Peluso D, Kanki K, Yang
728 Z *et al.* 2005. Deletion of active ADAMTS5 prevents cartilage degradation in a murine model of
729 osteoarthritis. *Nature* **434**: 644-648.

730 Groussin M, Mazel F, Sanders JG, Smillie CS, Lavergne S, Thuiller W, and Alm EJ. 2017. Unraveling the
731 processes shaping mammalian gut microbiomes over evolutionary time. *Nat Commun* **8**: 14319.

732 Grundler M, and Rabosky DL. 2020. Complex ecological phenotypes on phylogenetic trees: a Markov
733 process model for comparative analysis of multivariate count data. *Syst Biol* **69**: 1200-1211.

734 Hecker N, Sharma V, and Hiller M. 2019. Convergent gene losses illuminate metabolic and physiological
735 changes in herbivores and carnivores. *PNAS* **116**: 3036-3041.

736 Hooda J, Shah A, and Zhang L. 2014. Heme, an essential nutrient from dietary proteins, critically impacts
737 diverse physiological and pathological processes. *Nutrients* **6**: 1080-1102.

738 Hosseini-Alghaderi S, and Baron M. 2020. Notch3 in development, health and disease. *Biomolecules* **10**:
739 485.

740 Hou Y, Hu S, Li X, He W, and Wu G. 2020. Amino Acid Metabolism in the Liver: Nutritional and
741 Physiological Significance. In *Amino Acids in Nutrition and Health*. (ed. Wu G), pp. 21-37. Springer, Cham.

742 Hu Y, Wu Q, Ma S, T. M, Shan L, Wang X, Nie Y, Ning Z, Yan L, Xiu Y *et al.* 2017. Comparative
743 genomics reveals convergent evolution between the bamboo-eating giant and red pandas. *PNAS* **114**: 1081-
744 1086.

745 Hurrell R, and Egli I. 2010. Iron bioavailability and dietary reference values. *Am J Clin Nutr* **91**: 1461S-
746 1467S.

747 Ibar C, and Irvine KD. 2020. Integration of Hippo-YAP signaling with metabolism. *Dev Cell* **54**: 256-267.

748 Ishigame H, Kakuta S, Nagai T, Kadoki M, Nambu A, Komiyama Y, Fujikado N, Tanahashi Y, Akitsu A,
749 Kotaki H *et al.* 2009. Differential roles of interleukin-17A and -17F in host defense against mucoepithelial
750 bacterial infection and allergic responses. *Immunity* **30**: 108-119.

751 Izadi S, Aguilar de Soto N, Constantine R, and Johnson M. 2022. Feeding tactics of resident Bryde's whales
752 in New Zealand. *Mar Mammal Sci* **38**: 1104-1117.

753 Jain A, and Tuteja G. 2019. TissueEnrich: Tissue-specific gene enrichment analysis. *Bioinformatics* **35**:
754 1966-1967.

755 Jew S, AbuMweis SS, and Jones PJH. 2009. Evolution of the human diet: linking our ancestral diet to
756 modern functional foods as a means of chronic disease prevention. *J Med Food* **12**: 925-934.

757 Jia Y, Hwang SY, House JD, Ogborn MR, Weiler HA, Karmin O, and Aukema HM. 2010. Long-term high
758 intake of whole proteins results in renal damage in pigs. *J Nutr* **140**: 1646-1652.

759 Jordano P. 2000. Fruits and Frugivory. In *Seeds: the ecology of regeneration in plant communities*. 2nd ed.
760 (ed. Fenner M), pp. 125-166. CAB International, Wallingford, UK.

761 Julien-Laferrière D. 1999. Foraging strategies and food partitioning in the neotropical frugivorous
762 mammals *Caluromys philander* and *Potos flavus*. *J Zool* **247**: 71-80.

763 Karban R, and Agrawal AA. 2002. Herbivore offense. *Annu Rev Ecol Evol S* **33**: 641-664.

764 Kays RW. 1999. Food preferences of kinkajous (*Potos flavus*): a frugivorous carnivore. *J Mammal* **80**: 589-
765 599.

766 Kearney J. 2010. Food consumption trends and drivers. *Philos T R Soc B* **365**: 2793-2807.

767 Kim S, Cho YS, Kim H-M, Chung O, Kim H, Jho S, Seomun H, and Kim J. 2016. Comparison of carnivore,
768 omnivore, and herbivore mammalian genomes with a new leopard assembly. *Genome Biol* **17**: 211.

769 Kirilenko BM, Munegowda C, Osipova E, Jebb D, Sharma V, Blumer M, Morales A, Ahmed A,
770 Kontopoulos D, Hilgers L *et al.* 2023. Integrating gene annotation with orthology inference at scale. *Science*
771 **380**: eabn3107.

772 Ko G-J, Rhee CM, Kalantar-Zadeh K, and Joshi S. 2020. The effects of high-protein diets on kidney health
773 and longevity. *J Am Soc Nephrol* **31**: 1667-1679.

774 Konrad M, Hou J, Weber S, Dötsch J, Kari JA, Seeman T, Kuwertz-Bröking E, Peco-Antic A, Tasic V,
775 Dittrich K *et al.* 2008. *CLDN16* genotype predicts renal decline in familial hypomagnesemia with
776 hypercalciuria and nephrocalcinosis. *J Am Soc Nephrol* **19**: 171-181.

777 Kowalczyk A, Chikina M, and Clark NL. 2021. A cautionary tale on proper use of branch-site models to
778 detect convergent positive selection. bioRxiv doi: <https://doi.org/10.1101/2021.10.26.465984>

779 Kowalczyk A, Meyer WK, Partha R, Mao W, Clark NL, and Chikina M. 2019. RERconverge: an R package
780 for associating evolutionary rates with convergent traits. *Bioinformatics* **35**: 4815-4817.

781 Kowalczyk A, Partha R, Clark NL, and Chikina M. 2020. Pan-mammalian analysis of molecular constraints
782 underlying extended lifespan. *eLife* **9**: e51089.

783 Leung LLK, and Morser J. 2018. Carboxypeptidase B2 and carboxypeptidase N in the crosstalk between
784 coagulation, thrombosis, inflammation, and innate immunity. *J Thromb Haemost* **16**: 1474-1486.

785 Liberzon A, Subramanian S, Pinchback R, Thorvaldsdóttir H, Tamayo P, and Mesirov JP. 2011. Molecular
786 signatures database (MSigDB) 3.0. *Bioinformatics* **27**: 1739-1740.

787 Liu L, Lei T, Bankir L, Zhao D, Gai X, Zhao X, and Yang B. 2011. Erythrocyte permeability to urea and
788 water: comparative study in rodents, ruminants, carnivores, humans, and birds. *J Comp Physiol B* **181**: 65-
789 72.

790 Liu S, Lorenzen ED, Fumagalli M, Li B, Harris K, Xiong Z, Zhou L, Korneliussen TS, Somel M, Babbitt
791 C *et al.* 2014. Population genomics reveal recent speciation and rapid evolutionary adaptation in polar bears.
792 *Cell* **157**(4): 785-794.

793 Loerakker S, Stassen OMJA, ter Huurne FM, and Sahlgren CM. 2018. Mechanosensitivity of Jagged-Notch
794 signaling can induce a switch-type behavior in vascular homeostasis. *PNAS* **115**: E3682-E3691.

795 Lowe ME. 2002. The triglyceride lipases of the pancreas. *J Lipid Res* **43**: 2007-2016.

796 McCulloch DR, Nelson CM, Dixon LJ, Silver DL, Wylie JD, Lindner V, Sasaki T, Cooley MA, Argraves
797 WS, and Apte SS. 2009. ADAMTS metalloproteases generate active versican fragments that regulate
798 interdigital web regression. *Dev Cell* **17**: 687-698.

799 Mendes FK, and Hahn MW. 2016. Gene tree discordance causes apparent substitution rate variation. *Syst
800 Biol* **65**: 711-721.

801 Mendoza MLZ, Xiong Z, Escalera-Zamudio M, Runge AK, Thézé J, Streicker D, Frank H, K., Loza-Rubio
802 E, Liu S, Ryder OA *et al.* 2018. Hologenomic adaptations underlying the evolution of sanguivory in the
803 common vampire bat. *Nat Ecol Evol*: 659-668.

804 Morris SW, Kirstein MN, Valentine MB, Dittmer KG, Shapiro DN, Saltman DL, and Look AT. 1994.
805 Fusion of a kinase gene, ALK, to a nucleolar protein gene, NPM, in Non-Hodgkin's lymphoma. *Science*
806 **263**: 1281-1284.

807 Muegge BD, Kuczynski J, Knights D, Clemente JC, González A, Fontana L, Henrissat B, Knight R, and
808 Gordon JI. 2011. Diet drives convergence in gut microbiome functions across mammalian phylogeny and
809 within humans. *Science* **332**: 970-974.

810 Murrell B, Weaver S, Smith MD, Wertheim JO, Murrell S, Aylward A, Eren K, Pollner T, Martin DP,
811 Smith DM *et al.* 2015. Gene-wide identification of episodic selection. *Mol Biol Evol* **32**: 1365-1371.

812 Nowak RM. 1999. In *Walker's Mammals of the World*. 6th ed. Johns Hopkins University Press, Baltimore.

813 Okamoto N, Aruga S, Matsuzaki S, Takahashi S, Matsushita K, and Kitamura T. 2007. Associations
814 between renal sodium-citrate cotransporter (hNaDC-1) gene polymorphism and urinary citrate excretion in
815 recurrent renal calcium stone formers and normal controls. *Int J Urol* **14**: 344-349.

816 Orthofer M, Valsesia A, Mägi R, Wang Q-P, Kaczanowska J, Kozieradzki I, Leopoldi A, Cikes D, Zopf
817 LM, Tretiakov EO *et al.* 2020. Identification of ALK in thinness. *Cell* **181**: 1246-1262.

818 Pajor AM. 1999. Sodium-coupled transporters for Krebs cycle intermediates. *Annu Rev Physiol* **61**: 663-
819 682.

820 Palmer RH, Vernersson E, Grabbe C, and Hallberg B. 2009. Anaplastic lymphoma kinase: signalling in
821 development and disease. *Biochem J* **420**: 345-361.

822 Pang J-F, Kluetsch C, Zou X-J, Zhang A, Luo L-Y, Angleby H, Ardalan A, Ekström C, Sköllermo A,
823 Lundeberg J *et al.* 2009. mtDNA data indicate a single origin for dogs south of Yangtze river, less than
824 16,300 years ago, from numerous wolves. *Mol Biol Evol* **26**: 2849-2864.

825 Panthi S, Aryal A, Raubenheimer D, Lord J, and Adhikari B. 2012. Summer diet and distribution of the red
826 panda (*Ailurus fulgens fulgens*) in Dhorpatan Hunting Reserve, Nepal. *Zool Stud* **51**: 701-709.

827 Payne AH, and Hales DB. 2004. Overview of steroidogenic enzymes in the pathway from cholesterol to
828 active steroid hormones. *Endocr Rev* **25**: 947-970.

829 Pérez MM, Martins LMS, Dias MS, Pereira CA, Leite JA, Gonçalves ECS, de Almeida PZ, de Freitas EN,
830 Tostes RC, Ramos SG *et al.* 2018. Interleukin-17/interleukin-17 receptor axis elicits intestinal neutrophil
831 migration, restrains gut dysbiosis and lipopolysaccharide translocation in high-fat diet-induced metabolic
832 syndrome model. *Immunology* **156**: 339-355.

833 Pincu Y, Linden MA, Zou K, Baynard T, and Boppart MD. 2015. The effects of high fat diet and moderate
834 exercise on TGF β 1 and collagen deposition in mouse skeletal muscle. *Cytokine* **73**: 23-29.

835 Pineda-Munoz S, and Alroy J. 2014. Dietary characterization of terrestrial mammals. *Proc R Soc B* **281**:
836 20141173.

837 Pollard MD, and Puckett EE. 2022. Evolution of degrees of carnivory and dietary specialization across
838 Mammalia and their effects on speciation. bioRxiv doi: <https://doi.org/10.1101/2021.09.15.460515>

839 Pond SLK, Poon AFY, Velazquez R, Weaver S, Hepler NL, Murrell B, Shank SD, Magalis BR, Bouvier
840 D, Nekrutenko A *et al.* 2020. HyPhy 2.5—A customizable platform for evolutionary hypothesis testing
841 using phylogenies. *Mol Biol Evol* **37**: 295-299.

842 Pradhan S, Saha GK, and Khan JA. 2001. Ecology of the red panda *Ailurus fulgens* in the Singhalila
843 National Park, Darjeeling, India. *Biol Conserv* **98**: 11-18.

844 R Core Team. 2023. R: a language and environment for statistical computing. Vienna, Austria: R
845 Foundation for Statistical Computing.

846 Ranwez V, Douzery EJP, Cambon C, Chantret N, and Delsuc F. 2018. MACSE v2: Toolkit for the
847 alignment of coding sequences accounting for frameshifts and stop codons. *Mol Biol Evol* **35**: 2582-2584.

848 Reuter DM, Hopkins SSB, and Price SA. 2023. What is a mammalian omnivore? Insights into terrestrial
849 mammalian diet diversity, body mass and evolution. *P R Soc B* **290**: 20221062.

850 Revell LJ. 2012. phytools: an R package for phylogenetic comparative biology (and other things). *Methods
851 Ecol Evol* **3**: 317-223.

852 Robertson WG, Heyburn PJ, Peacock M, and Swaminathan R. 1979. The effect of high animal protein
853 intake on the risk of calcium stone formation in the urinary tract. *Clin Sci* **57**: 285-288.

854 Russell DW. 2003. The enzymes, regulation, and genetics of bile acid synthesis. *Annu Rev Biochem* **72**:
855 137-174.

856 Saputra E, Kowalczyk A, Cusick L, Clark N, and Chikina M. 2021. Phylogenetic permutations: a
857 statistically rigorous approach to measure confidence in associations in a phylogenetic context. *Mol Biol
858 Evol* **38**: 3004-3021.

859 Savolainen P, Zhang Y-P, Luo J, Lundeberg J, and Leitner T. 2002. Genetic evidence for an East Asian
860 origin of domestic dogs. *Science* **298**: 1610-1613.

861 Schermerhorn T. 2013. Normal glucose metabolism in carnivores overlaps with diabetes pathology in non-
862 carnivores. *Front Endocrinol* **4**: 188.

863 Schliep KP. 2011. phangorn: phylogenetic analysis in R. *Bioinformatics* **27**: 592-593.

864 Simon DB, Lu Y, Choate KA, Velazquez H, Al-Sabban E, Praga M, Casari G, Bettinelli A, Colussi G,
865 Rodriguez-Soriano J *et al.* 1999. Paracellin-1, a renal tight junction protein required for paracellular Mg²⁺
866 resorption. *Science* **285**: 103-106.

867 Smith CL, Goldsmith CW, and Eppig JT. 2005. The Mammalian Phenotype Ontology as a tool for
868 annotating, analyzing and comparing phenotypic information. *Genome Biol* **6**: R7.

869 Soligo C, and Martin RD. 2006. Adaptive origins of primates revisited. *J Hum Evol* **50**: 414-430.

870 Sponheimer M, and Lee-Thorp JA. 1999. Isotopic evidence for the diet of an early hominid,
871 *Australopithecus africanus*. *Science* **283**: 368-370.

872 Stamatakis A. 2014. RAxML version 8: a tool for phylogenetic analysis and post-analysis of large
873 phylogenies. *Bioinformatics* **30**: 1312-1313.

874 Storey JD, Bass AJ, Dabney A, and Robinson D. 2020. qvalue: Q-value estimation for false discovery rate
875 control. <http://github.com/jdstorey/qvalue>.

876 The GTEx Consortium. 2015. The Genotype-Tissue Expression (GTEx) pilot analysis: Multitissue gene
877 regulation in humans. *Science* **348**: 648-660.

878 Tovar-Palacio C, Tovar AR, Torres N, Cruz C, and Hernández-Pando R. 2011. Proinflammatory gene
879 expression and renal lipogenesis are modulated by dietary protein content in obese Zucker ^{fa/fa} rats. *Am J
880 Physiol-Renal* **300**: F263-F271.

881 Upham NS, Esselstyn JA, and Jetz W. 2019. Inferring the mammal tree: Species-level sets of phylogenies
882 for questions in ecology, evolution, and conservation. *PLoS Biol* **17**: e3000494.

883 Vincze O, Colchero F, Lemaître J-F, Conde DA, Pavard S, Bieuville M, Urrutia AO, Ujvari B, Boddy AM,
884 Maley CC *et al.* 2021. Cancer risk across mammals. *Nature* **601**: 263-267.

885 Wagner F, Ruf I, Lehmann T, Hofmann R, Ortmann S, Schiffmann C, Hiller M, Stefen C, and Stuckas H.
886 2022. Reconstruction of evolutionary changes in fat and toxin consumption reveals associations with gene
887 losses in mammals: a case study for the lipase inhibitor *PNLIPRP1* and the xenobiotic receptor *NR1I3*. *J
888 Evol Biol* **35**: 225-239.

889 Wang LW, Dlugosz M, Somerville RPT, Raed M, Haltiwanger RS, and Apte SS. 2007. O-fucosylation of
890 thrombospondin type 1 repeats in ADAMTS-like-1/punctin-1 regulates secretion. *J Biol Chem* **282**: 17024-
891 17031.

892 Wang Z, Xu S, Du K, Huang F, Chen Z, Zhou K, Ren W, and Yang G. 2016. Evolution of digestive enzymes
893 and RNASE1 provides insights into dietary switch of cetaceans. *PLoS Biol* **13**: 3144-3157.

894 Wertheim JO, Murrell B, Smith MD, Kosakovsky Pond SL, and Scheffler K. 2015. RELAX: Detecting
895 relaxed selection in a phylogenetic framework. *Mol Biol Evol* **32**: 820-832.

896 Williams AS, Kang L, and Wasserman DH. 2015. The extracellular matrix and insulin resistance. *Trends
897 Endocrin Met* **26**: 357-366.

898 Wilman H, Belmaker J, Simpson J, de la Rosa C, Rivadeneira MM, and Jetz W. 2014. Elton Traits 1.0:
899 Species-level foraging attributes of the world's birds and mammals. *Ecology* **95**: 2027.

900 Wirthlin ME, Schmid TA, Elie JE, Zhang X, Kowalczyk A, Redlich R, Shvareva VA, Rakuljic A, Ji MB,
901 Bhat NS *et al.* 2024. Vocal learning-associated convergent evolution in mammalian proteins and regulatory
902 elements. *Nature* **383**: eabn3263.

903 Worth CL, Gong S, and Blundell TL. 2009. Structural and functional constraints in the evolution of protein
904 families. *Nat Rev Mol Cell Bio* **10**: 709-720.

905 Wu Y. 2022. Diet evolution of carnivorous and herbivorous mammals in Laurasiatheria. *BMC Ecol Evol*
906 **22**: 82.

907 Yang Z. 2007. PAML 4: phylogenetic analysis by maximum likelihood. *Mol Biol Evol* **24**: 1586-1591.

908 Yonzon PB, and Hunter ML. 1991. Conservation of the red panda *Ailurus fulgens*. *Biol Conserv* **57**: 1-11.

909 Yu G, and He Q-Y. 2016. ReactomePA: an R/Bioconductor package for reactome pathway analysis and
910 visualization. *Mol BioSyst* **12**: 477-479.

911 Yu G, Wang L-G, Han Y, and He Q-Y. 2012. clusterProfiler: an R package for comparing biological themes
912 among gene clusters. *OMICS* **16**: 284-287.

913 Zoelzer F, Burger AL, and Dierkes PW. 2021. Unraveling differences in fecal microbiota stability in
914 mammals: from high variable carnivores and consistently stable herbivores. *Anim Microbiome* **3**: 77.

915 Zoonomia Consortium. 2020. A comparative genomics multitool for scientific discovery and conservation.
916 *Nature* **587**: 240-245.

917